

Published in final edited form as:

ACS Nano. 2010 January 26; 4(1): 199. doi:10.1021/nn901256s.

Synthetic Polymer Nanoparticles with Antibody-Like Affinity for a Hydrophilic Peptide

Zhiyang Zeng, Yu Hoshino, Andy Rodriguez, Hoseong Yoo, and Kenneth J. Shea

Department of Chemistry, University of California, Irvine. CA 92697 USA

Abstract

Synthetic polymer nanoparticles with antibody-like affinity for a hydrophilic peptide have been prepared by inverse microemulsion polymerization. Peptide affinity was achieved in part by incorporating the target (imprint) peptide in the polymerization reaction mixture. Incorporation of the imprint peptide assists in the creation of complementary binding sites in the resulting polymer nanoparticle (NP). To orient the imprint peptide at the interface of the water and oil domains during polymerization, the peptide target was coupled with fatty acid chains of varying length. The peptide-NP binding affinities (90 nM~900 nM) were quantitatively evaluated by a quartz crystal microbalance (QCM). The optimal chain length was established that created high affinity peptide binding sites on the *surface* of the nanoparticles. This method can be used for the preparation of nanosized synthetic polymers with antibody-like affinity for hydrophilic peptides and proteins (“plastic antibodies”).

Keywords

Selective peptide capture; Synthetic nanoparticles; Molecular imprinting; QCM; Inverse microemulsion polymerization; Plastic antibodies

There is considerable need for functional materials with selective affinity for specific peptide sequences and proteins. Such materials can be used as platforms for drug delivery, biosensors, biomedical diagnostics and for therapeutics. There are few general strategies for the creation of synthetic receptors. These include aptamer and phage display techniques that generate libraries of synthetic oligonucleotides/peptides.¹⁻² A screening assay is then employed to identify candidate receptor ligands. The nonbiological approach of molecular imprinting creates populations of specific recognition sites in synthetic network polymers. Binding sites result from polymerization of cross-linking and functional monomers in the presence of an imprinting molecule.³⁻⁹ Historically, molecularly imprinted polymers (MIPs) have been prepared in aprotic solvents against small hydrophobic organic molecules. More recently, there have been efforts to extend imprinting to biological macromolecules.¹⁰⁻¹² These include reports of peptide/protein-imprinted polymers prepared by bulk polymerization and surface imprinted polymer films. In some cases materials with sub micromolar polymer-protein affinity were obtained.¹³ Nanoparticles (NPs) offer a greater number of end-use applications and the potential for higher capture capacity than bulk materials and films. The NP format expands opportunities for applications such as synthetic substitutes for natural antibodies.¹⁴⁻¹⁷ In a few examples reported, antibody-like affinity has been obtained. We have reported the preparation of synthetic polymer nanoparticles (“plastic antibodies”) against a twenty-six amino acid peptide, melittin.¹⁴ A precipitation polymerization method was employed for the nanoparticle

Address correspondence to kjshea@uci.edu.

Supporting Information Available: Quantification of removal of surfactants, SEM image of NPs, Langmuir binding isotherm of MIP (C15-P) to GFP-9 and competitive study of free GFP-9.

(NP) synthesis. As the polymer forms from a homogeneous aqueous solution, it undergoes a phase separation.^{18–19} It was proposed that the amphiphilic imprint peptide (melittin) locates at the interface of the polymer-aqueous domain. At this location, the melittin can assist in the organization of the developing polymer and creation of complementary binding sites. This model proposes the binding sites are created on the *surface* of the NPs due to melittin's amphiphilic nature. As with natural antibodies, binding domains are at or near the surface of the protein and thus easily accessible. The preceding technique (precipitation polymerization) was found to be successful for amphiphilic peptides. However, many hydrophilic biomacromolecules including peptides, carbohydrates and proteins would not be suitable candidates for this approach since the target or imprint peptide would have little bias to locate at the developing water-polymer interface during polymerization. In this report we describe a method for the fabrication of synthetic polymer NPs with surface binding sites for *hydrophilic peptides*. The approach utilizes inverse microemulsion polymerization coupled with a modified hydrophilic peptide imprint molecule to synthesize nanoparticles with high affinity for the target peptide. The procedure provides a general strategy for preparing synthetic polymer NPs with high affinity for hydrophilic peptides.

Results and Discussion

For this work, the peptide (**GFP-9**: H-THGMDELYK-OH, $M_w=1092$ Da) sequence was chosen as the hydrophilic peptide target. It corresponds to the unstructured exposed C-terminus of Green Fluorescent Protein (GFP). The peptide contains more than 50% hydrophilic amino acid residues. As such, it can serve as a model for designing and fabricating synthetic NPs with sequence specificity for unstructured hydrophilic peptides. Evaluation of available polymerization methods led to inverse microemulsion polymerization^{20–24} as the method of choice for this particular challenge. Inverse microemulsion polymerization entails an aqueous solution of monomers dispersed in nano-sized droplets in an immiscible organic solvent. The droplets are stabilized by surfactants. If a hydrophilic peptide is to be used as an imprint molecule, the peptide will be restricted to the nano-sized water domain. This is in contrast to precipitation polymerization where the peptide is dispersed in a large volume of water. It was anticipated that inverse microemulsion polymerization would result in a significantly higher imprinting efficiency for hydrophilic peptide targets.

For NPs designed to capture peptide and protein targets, the accessibility of binding sites is important. To ensure that the peptide remains at the interface of the water and oil domains during polymerization, the peptide was coupled with fatty acid chains at the N-terminus by amide coupling (Fig 1a). Ideally, the modified peptides can function as surfactant molecules, with the hydrophobic head in the oil layer and the hydrophilic peptide at the surface of the aqueous domain which contains the monomers. The peptide is in position to assist in the organization of the growing polymer NP in the aqueous droplet where the polymerization is taking place. In this study we included modified peptides with hydrocarbon tails of 5, 13 and 15 carbons to establish the importance of orienting the peptide at the interface and to determine the requirements for achieving that goal.

In a typical NP preparation, an aqueous monomer solution (acrylamide, 28.5 wt%; N, N'-ethylene bisacrylamide, 8.2 wt%) was dispersed into hexane with surfactants (AOT and Brij 30) (Fig 1b). Modified peptides (1 mg) were added to the microemulsion. Solutions were stirred for 1 h. The polymerization was initiated at room temperature upon addition of ammonium persulfate (APS) and N,N,N',N'-tetramethylethylenediamine (TEMED). The solution became bluish during polymerization over 2h. The polymer NPs were washed with ethanol followed by dialysis against water for 7 days to remove the surfactants, unreacted monomers and peptide (Supporting Information Figure S1). Imprinted NPs were identified as **MIP (C5-P)**, **MIP (C13-P)** and **MIP (C15-P)** depending on the length of the hydrophobic tail of the modified peptides.

Control, non-imprinted NPs (**NIP**) was prepared under identical conditions in the absence of added peptide. **MIP** NPs and **NIP** NPs were determined to be approximately 28 nm in size by DLS and spherical in shape by SEM (Fig 1c and Supporting Information Figure S2). Further confirmation of surfactant removal in the dialysis step was obtained by monitoring the zeta potential. Following dialysis the NPs had negligible surface charge (Supporting Information Table S1).

A 27 MHz quartz crystal microbalance (QCM)^{25–26} was used to quantify interactions between NPs and **GFP-9**. In order to reduce the non-specific binding, the gold surface of the QCM sensor was functionalized with an oligo ethylene glycol (OEG) alkanethiol mixed SAM (7:3 HS(CH₂)₁₁OEG₃OH:HS(CH₂)₁₁OEG₆COOH).²⁷ Peptides were immobilized on the SAM layer by amide coupling of the N-terminal amine of **GFP-9** to the carboxylate end of the SAM (Fig. 2a). A representative time course of frequency changes of the 27 MHz QCM is shown in Fig 2b. NPs solutions were injected into the sensor cells at the indicated intervals. The frequency change is inversely proportional to the mass increase on the sensor. It is noted that there is a substantial frequency decrease in response to the injection of **MIP (C13-P)** and **MIP (C15-P)** when compared to that of the **NIP**. Interestingly, little mass change was detected upon injection of **MIP (C5-P)**. Based on the interactions with the **GFP-9** peptide, four NPs thus were categorized into two groups: NPs with a strong affinity for the peptide including **MIP (C13-P)** and **MIP (C15-P)** and polymer nanoparticles with little or no affinity for the peptide. The latter group includes **MIP (C5-P)** and **NIP** (Fig 2c).

In order to confirm that the mass change was due to the interaction between NPs and **GFP-9**, three control experiments were carried out on **MIP (C15-P)** and **NIP** (Fig 3). For the first control, a SAM surface without immobilization of a peptide was used. **MIP (C15-P)** and **NIP** were injected into two separate sensor cells. No difference in mass change was observed for both NPs and the mass changes were almost identical to the **GFP-9** modified surface with **NIP**. For the second control experiment, **peptide A** (H-AYLKKATNE-OH, MW=1038 Da) with molecular weight and composition similar to **GFP-9** was immobilized onto the SAM surface in place of **GFP-9** and the interactions with **MIP (C15-P)** and **NIP** were tested. Once again there was no difference in the interaction of **MIP (C15-P)** and **NIP** with the surface. One final control experiment involved NP competition between surface bound and free peptide (Fig 3b and Supporting Information Figure 4). When a solution of **GFP-9** (0.1 mM) was incubated with **MIP (C15-P)** QCM analysis of the resulting solution revealed a significant reduction in binding to the surface bound peptide (60 Hz frequency decrease compared to 200Hz for the **MIP (C15-P)** NP without free **GFP-9**).

The first control experiment with the oligo ethylene glycol (OEG) alkanethiol mixed SAM surface suggested that both NPs have a slight non-specific affinity to the PEG/carboxylated surface. The interaction is similar to that between **NIP** and **GFP-9**. The large mass changes upon injection of **MIP (C15-P)** to **GFP-9** surfaces therefore are due to the interaction between **MIP (C15-P)** and **GFP-9** peptide. The apparent disassociation constant K_d , of **MIP (C15-P)** to **GFP-9**, which was obtained by fitting the binding plots to the Langmuir adsorption isotherm, is estimated to be within 90 nM~900 nM. (Supporting Information Figure S3). The second control experiment using the non-target **peptide A** immobilized on the QCM surface, establishes that **MIP(C15-P)** has a high affinity only to the specific peptide sequence for which it was imprinted and exhibits relatively low levels of non-specific binding to other peptide sequences even if the composition of two peptides share similarities. This finding is consistent with earlier reports of peptide imprinted polymer films¹³ of similar chemical composition and confirms this technique as a means for creating selective peptide receptor sites with nanomolar affinity. The last control experiment demonstrated that free **GFP-9** in solution can competitively inhibit the interaction between the **MIP-NP** and **GFP-9** immobilized on the QCM

sensor surface. This would be expected if the basis of the surface interaction was due to NP-peptide binding.

Synthetic polymer nanoparticles with high affinity and selectivity for the hydrophilic peptide HTHGMDELKY-OH (**GFP-9**) were prepared by inverse microemulsion polymerization. The peptide was coupled with three different fatty acids in an effort to orientate the peptide at the interface of water and oil domains. The NP-peptide binding data call attention to the importance of tuning the properties of the imprinting peptide for successful surface imprinting of hydrophilic peptides. NPs imprinted with **C13-P** or **C15-P** strongly bind the **GFP-9** peptide while NPs imprinted with **C5-P** do not. We attribute this to differences in the partitioning of the modified peptides in the microemulsion. We propose that **C13-P** and **C15-P** are located primarily at the water-oil interface and **C5-P** is dispersed more uniformly throughout the aqueous droplet. Support for this comes from the solution behavior of the three modified peptides. **C5-P** readily dissolves in aqueous solution. However, **C13-P** and **C15-P** do not (Fig. 4a). When peptides were added to the mixture of water and hexane, **C13-P** and **C15-P** form emulsions; **C5-P** on the other hand does not (Fig 4b). In the polymerization reaction, **C13-P** and **C15-P** are more likely to remain at the water/oil interface while most of **C5-P** would partition in the water phase. Following polymerization, binding sites are created at or near the surface of **MIP (C13-P)** and **MIP (C15-P)** but are created in the interior of **MIP (C5-P)**. The QCM data is consistent with this analysis. For the QCM experiments, **GFP-9** was immobilized on the SAM surface. Only those binding sites on or near the surface of the NPs would be accessible to the immobilized peptide. Little interaction is observed between **MIP (C5-P)** and **GFP-9**. NPs prepared in the absence of added peptide (**NIP**), also showed little interaction with **GFP-9**, similar to the behavior of **MIP (C5-P)**. The similarities between **MIP (C5-P)** and **NIP** support our proposal that **C5-P** does not orient at the interface during polymerization.

We attribute the interaction between **MIP (C15-P)** and **GFP-9** peptide to multiple hydrogen bonding interactions. Acrylamide and N, N'-ethylene bisacrylamide can function as both a hydrogen bond donor and acceptor. We suggest that during the polymerization, these monomers interact with **GFP-9** by multiple weak hydrogen bonds to generate a distribution of complementary sites in the resulting NP. The cumulative effect of multiple weak hydrogen bonds can lead to a polymer NP with a population of binding sites with strong specific interactions for the target (imprinted) peptide. Following removal of imprint peptide, binding sites on the surface of the NPs with nanomolar affinity are achieved. Although rigorous analysis of the binding isotherms of imprinted polymers reveals a distribution of binding site affinities,³ under ideal conditions (*i.e.* low concentration) this small population of high affinity sites has noteworthy affinity and selectivity.

In summary, we have developed a strategy to create synthetic polymer NPs with antibody-like affinity for a hydrophilic peptide using inverse microemulsion polymerization. By surveying peptides with fatty acid chains of varying length, conditions were found to “fix” the peptide at the droplet interface. Subsequent polymerization of the droplet resulted in a polymer NP with nanomolar affinity and high specificity for the target peptide. This approach may be used not only for the design of synthetic “polymer antibodies” for peptides, and also proteins using an epitope imprinting approach.^{13,28} These results will be reported in a future report.

METHOD

Materials

Acrylamide, Dioctyl sulfosuccinate, sodium salt (AOT), ammonium persulfate (APS), N,N,N',N'-tetramethylethylenediamine (TEMED), N-(3-Dimethylaminopropyl)-N'-ethylcarbodiimide hydrochloride (EDC) were purchased from Sigma-Aldrich, USA. Brij30 was purchased from ACROS Organic, USA. N-hydroxysuccinimide (NHS) was from Fluka.

HS(CH₂)₁₁EG₆COOH was purchased from SensoPath Technologies, Inc. Peptide **C5-P**, **C13-P** and **C15-P** were purchased from Genemed Synthesis, Inc., USA (98% purity). **Peptide A**, **GFP-9** were purchased from Peptide Support Ltd, Japan (98% purity). All chemicals were used as received. N,N'-ethylenebisacrylamide²⁹ and HS(CH₂)₁₁EG₃OH³⁰ were prepared according to literature procedures. Water used in polymerization and characterization was distilled then purified using a Barnstead Nanopure Diamond™ system.

Preparation of NPs

A monomer solution was prepared by adding acrylamide (0.45 g, 6.3 mmol) and ethylene-bisacrylamide (0.13 g, 0.77 mmol) to water (1.0 mL). Then 1.0 mL of the monomer solution was added dropwise to a deoxygenated solution of hexanes (21.5 mL), AOT (0.8 g) and Brij 30 (1.54 g). The solution was stirred continuously during the additions. GFP-9 modified peptide (**C5-P**, **C13-P** or **C15-P**, 1 mg) was then added to the mixture. The microemulsion was stirred for 1 h. To initiate the polymerization, ammonium persulfate solution (30 μL of 10% (w/v)) and TEMED (15 μL) were added. The solution was stirred at room temperature for 2 h to assure complete polymerization. In order to remove unreacted monomers, peptide and surfactants, ethanol (40 mL) was added to precipitate the nanoparticle followed by centrifugation at 5000 RPM for 30 min. The nanoparticles were washed with EtOH (4X), and resuspended into 10% AcOH in water. The suspension was dialyzed against a large excess of water (2X daily changes) for 7 days. The preparation of non-imprinted nanoparticles was exactly the same as the preparation of imprinted nanoparticles, except peptide was not added. The yield of NPs was determined by measuring the weight of a lyophilized aliquot of NP solution following dialysis. Yields of the four NPs after purification were approximately 50%.

Size and Zeta Potential Measurements

The hydrodynamic radius, as well as zeta potential, of the purified NPs was determined by a ZEN3600 Zetasizer (Malvern Instruments Ltd) which uses a 4mW 633 nm He-Ne laser. Data was collected at a fixed scattering angle of 90° at 25°C. NPs (1 mg/mL) were sonicated for 5 min before each measurement. A minimum of three measurements were taken and averaged for each NP.

SEM Image

A drop of nanoparticle suspension (1 mg/mL) was added to the silicon wafer and dried overnight. The nanoparticles were coated with iridium before imaging. A ZEISS ULTRA 55 CDS ultra-high-resolution field-emission scanning electron microscope (FE-SEM) was used in this study.

Monitoring NP-Peptide Interactions in Real-Time by Quartz Crystal Balance (QCM)

An Affinix Q4 QCM was used (Initium Co. Ltd, Tokyo, <http://www.initium2000.com>). The instrument has four 500 μL cylindrical cells (10 mm i.d.) each equipped with a 27 MHz QCM plate (8 mm diameter quartz plate and 4.9 mm² Au electrode) at the bottom of the cell and a horizontal mixer with temperature-control.

Immobilization of GFP-9 peptide

To a clean gold sensor was added an OEG alkanethiol mixture (0.1 mM 7:3 HS (CH₂)₁₁OEG₃OH : HS(CH₂)₁₁OEG₆COOH in 50/50 EtOH/Water solution). The cell was incubated overnight. Sensor cells were rinsed with water (10 X). EDC (100 μL of 100 μg/mL) and NHS (100 mg/mL) were added to the cells. After 20 min the cells were washed with water (10 X). NaAc buffer (pH=4.2) was then added. GFP-9 in water (2 μL of 10 mg/mL) was injected into QCM sensor cells and allowed to incubate overnight. The immobilization of peptide was monitored by QCM.

Interaction Between Peptide and Nanoparticles

PBS buffer (10 mM PBS, 150 mM NaCl, 0.005% Tween20) was used throughout the study. The baseline was equilibrated for 2 h until the frequency change was within ± 1 Hz/30min. Nanoparticle solutions were injected into the cells and the frequency change was monitored.

Supplementary Material

Refer to Web version on PubMed Central for supplementary material.

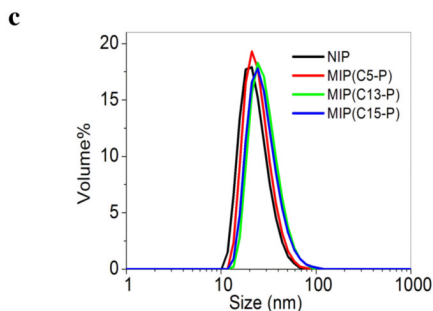
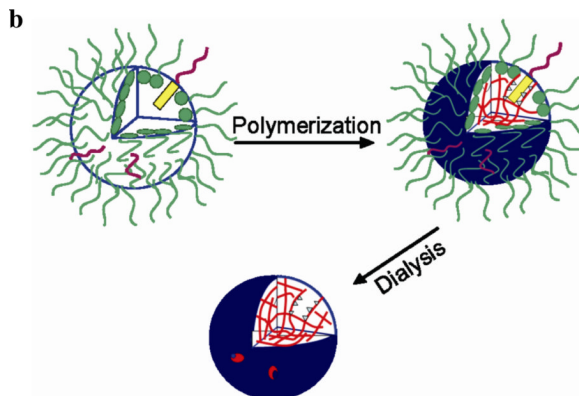
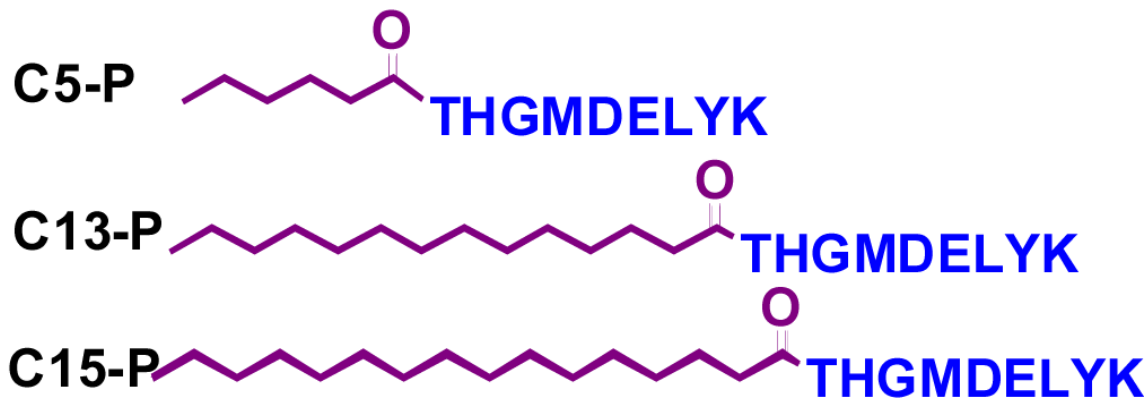
Acknowledgments

We thank T. Ozeki at Initium, Inc. for assistance with the QCM measurement as well as Dr. Wytze van der Veer (Department of Chemistry, UCI) for the help with the DLS measurements. We also thank Yen Peng Kong (Department of Chemical Engineering and Materials Science, UCI) for assistance with the SEM measurement. Financial support from the National Institutes of Health is gratefully acknowledged.

REFERENCES

1. Smith GP, Petrenko VA. Phage Display. *Chem. Rev* 1997;97:391–410. [PubMed: 11848876]
2. Mayer G. The Chemical Biology of Aptamers. *Angew. Chem., Int. Ed* 2009;48:2672–2689.
3. Yan, M.; Ramstrom, O., editors. *Molecularly Imprinted Materials: Science and Technology*. CRC press; 2004.
4. Wulff G. Molecular Imprinting in Cross-Linked Materials with the Aid of Molecular Templates- A Way towards Artificial Antibodies. *Angew. Chem., Int. Ed* 1995;34:1812–1832.
5. Mosbach K. The Promise of Molecular Imprinting. *Sci. Am* 2006;295:86–91. [PubMed: 16989485]
6. Zimmerman SC, Lemcoff NG. Synthetic Hosts via Molecular Imprinting—Are Universal Synthetic Antibodies Realistically Possible? *Chem. Commun* 2004:5–14.
7. Sellergren, B., editor. *Molecularly Imprinted Polymers*. Elsevier; Amsterdam: 2001.
8. Shea K. Molecular Imprinting of Synthetic Network Polymers. *Trends Polym. Sci* 1994;2:166–173.
9. Hart BR, Shea K. Synthetic Peptide Receptors: Molecularly Imprinted Polymers for the Recognition of Peptides Using Peptide-Metal Interactions. *J. Am. Chem. Soc* 2001;123:2072. [PubMed: 11456837]
10. Hansen DE. Recent Developments in the Molecular Imprinting of Proteins. *Biomaterials* 2007;28:4178–4191. [PubMed: 17624423]
11. Janiak DS, Kofinas P. Molecular Imprinting of Peptides and Proteins in Aqueous Media. *Anal. Bioanal. Chem* 2007;389:399–404.
12. Turner NW, Jeans CW, Brain KR, Allender CJ, Hlady V, Britt DW. From 3D to 2D: A Review of the Molecular Imprinting of Proteins. *Biotechnol. Prog* 2006;22:1474–1489. [PubMed: 17137293]
13. Nishino H, Huang C-S, Shea K. Selective Protein Capture by Epitope Imprinting. *Angew. Chem. Int. Ed* 2006;45:2392–2396.
14. Hoshino Y, Kodama T, Okahata Y, Shea K. Peptide Imprinted Polymer Nanoparticles: A Plastic Antibody. *J. Am. Chem. Soc* 2008;130:15242–15243. [PubMed: 18942788]
15. Li Y, Yang HH, You QH, Zhuang ZX, Wang XR. Protein Recognition via Surface Molecularly Imprinted Polymer Nanowires. *Anal. Chem* 2006;78:317–320. [PubMed: 16383343]
16. Tan CJ, Wangrangsamakul S, Bai R, Tong YW. Defining the Interactions between Proteins and Surfactants for Nanoparticle Surface Imprinting through Miniemulsion Polymerization. *Chem. Mater* 2008;20:118–127.
17. Flavin K, Resmini M. Imprinted Nanomaterials: A New Class of Synthetic Receptors. *Anal. Bioanal. Chem* 2009;393:437–444. [PubMed: 19023566]
18. Pelton R. Temperature-sensitive Aqueous Microgels. *Adv. Colloid. Interfac* 2000;85:1–33.
19. Debord JD, Lyon LA. Synthesis and Characterization of pH-Responsive Copolymer Microgels with Tunable Volume Phase Transition Temperatures. *Langmuir* 2003;19:7662–7664.

20. Candau F, Leong YS, Pouyet G, Candau S. Inverse Microemulsion Polymerization of Acrylamide: Characterization of the Water-in-Oil Microemulsions and the Final Microlatexes. *J. Colloid. Interf. Sci* 1984;101:167–183.
21. Daubresse C, Grandfils C, Jerome R, Teyssie P. Enzyme Immobilization in Nanoparticles Produced by Inverse Microemulsion Polymerization. *J. Colloid. Interf. Sci* 1994;168:222–229.
22. Clark HA, Kopelman R, Tjalkens R, Philbert MA. Optical Nanosensors for Chemical Analysis inside Single Living Cells. 1. Fabrication, Characterization, and Methods for Intracellular Delivery of PEBBLE Sensors. *Anal. Chem* 1999;71:4837–4843. [PubMed: 10565275]
23. McAllister K, Peter S, Adam M, Cho MJ, Rubinstein M, Samulski RJ, DeSimone JM. Polymeric Nanogels Produced via Inverse Microemulsion Polymerization as Potential Gene and Antisense Delivery Agents. *J. Am. Chem. Soc* 2002;124:15198–15207. [PubMed: 12487595]
24. Antonietti M. Microgels- Polymers with a Special Molecular Architecture. *Angew. Chem. Int. Ed* 1988;27:1743–1747.
25. Matsuno H, Furusawa H, Okahata Y. Kinetic Study of Phosphorylation-Dependent Complex Formation between the Kinase-Inducible Domain (KID) of CREB and the KIX Domain of CBP on a Quartz Crystal Microbalance. *Chem. Eur. J* 2004;10:6172–6178.
26. Hoshino Y, Kawasaki T, Okahata Y. Effect of Ultrasound on DNA Polymerase Reactions: Monitoring on a 27-MHz Quartz Crystal Microbalance. *Biomacromol* 2006;7:682–685.
27. Lahiri J, Isaacs L, Tien J, Whitesides GM. A Strategy for the Generation of Surfaces Presenting Ligands for Studies of Binding Based on an Active Ester as a Common Reactive Intermediate: A Surface Plasmon Resonance Study. *Anal. Chem* 1999;71:777–790. [PubMed: 10051846]
28. Rachkov A, Minoura N. Recognition of Oxytocin and Oxytocin-related Peptides in Aqueous Media Using a Molecularly Imprinted Polymer Synthesized by the Epitope Approach. *J. Chromatogr. A* 2000;889:111–118. [PubMed: 10985543]
29. Shea KJ, Stoddard GJ, Shavelle DM, Wakui F, Choate RM. Synthesis and Characterization of Highly Crosslinked Poly(acrylamides) and Poly(methacrylamides). A New Class of Macroporous Polyamides. *Macromolecules* 1990;23:4497–4507.
30. Pale-Grosdemange C, Simon ES, Prime KL, Whitesides GM. Formation of Self-Assembled Monolayers by Chemisorption of Derivatives of Oligo(ethylene glycol) of Structure $\text{HS}(\text{CH}_2)_{11}(\text{OCH}_2\text{CH}_2)_m\text{OH}$ on Gold Formation of Self-Assembled Monolayers by Chemisorption of Derivatives of Oligo(ethylene glycol) of Structure $\text{HS}(\text{CH}_2)_{11}(\text{OCH}_2\text{CH}_2)_m\text{OH}$ on Gold. *J. Am. Chem. Soc* 1991;113:12–20.

a**Figure 1.**

Preparation of hydrophilic imprinted NPs by inverse microemulsion polymerization. (a) Peptides utilized in this study: **C5-P**, **C13-P** and **C15-P**. The peptide was coupled with fatty acids (five, thirteen and fifteen carbons) at the N-terminus. (b) Schematic of the preparation of imprinted NPs. An aqueous monomer solution was dispersed into nano-sized water droplets in hexane. The droplets were stabilized by the surfactants AOT and Brij30 (Green). Modified peptides (yellow) were added into the microemulsion. The polymer nanoparticles (dark blue) were formed by addition of APS/TEMED initiator. Processing consisted of washing with EtOH and dialysis against water. (c) Size distribution of the three imprinted NPs and a control non-imprinted nanoparticle (NIP) as determined by DLS. Spectra of the NPs (1mg/mL) were taken in water after dialysis. Three measurements were taken and averaged for each NP.

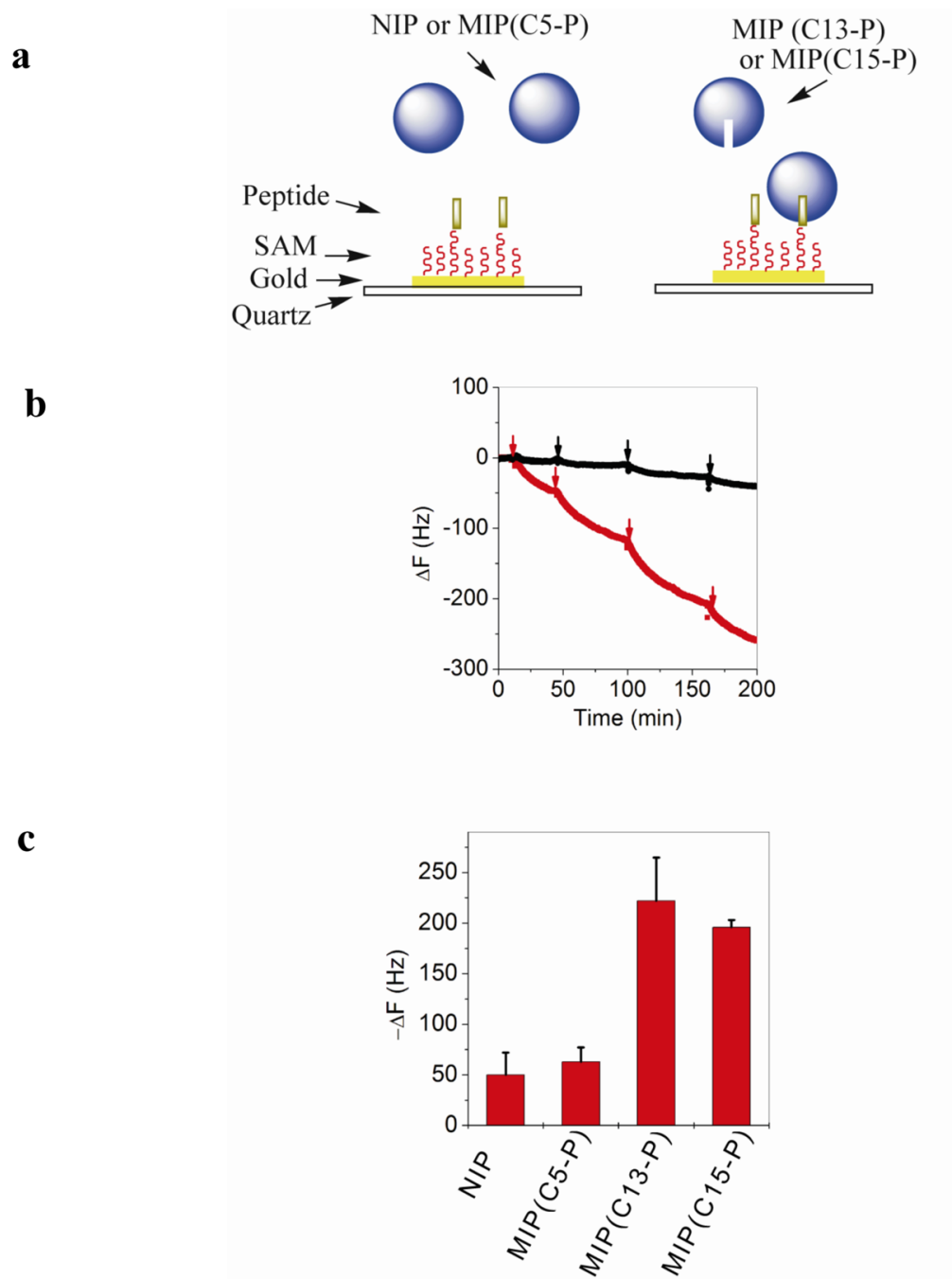


Figure 2. Interaction between nanoparticles and immobilized peptide by QCM. (a) Schematic of QCM experiments for monitoring interactions between NPs (left: **NIP** or **MIP(C5-P)** and right: **MIP(C13-P)** or **MIP(C15-P)**) and **GFP-9** peptide immobilized on QCM electrode. (b) Representative time courses of frequency change of the 27 MHz QCM. **GFP-9** peptide was immobilized on the QCM electrode. Solutions of **MIP(C5-P)** (black line) and **MIP(C13-P)** (red line) were injected at the time points indicated by the arrows into two separate QCM cells. (c): Frequency Shift upon injections of **NIP**, **MIP(C5-P)**, **MIP(C13-P)** and **MIP(C15-P)** to QCM sensor cells with **GFP-9** immobilized on the surface. Data represent the mean frequency

change \pm standard deviation (n=3) after injection of 64 $\mu\text{g}/\text{mL}$ polymeric NP solutions in **GFP-9**-immobilized QCM cells.

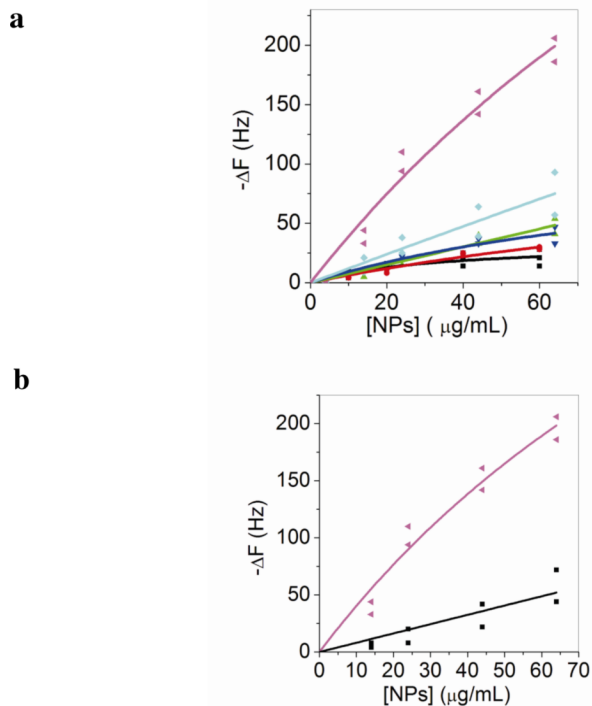


Figure 3.

(a) Binding isotherms of **MIP (C15-P)-GFP-9** (pink line) and **NIP-GFP-9** (cyan line), **MIP (C15-P)-SAM** (green line) and **NIP-SAM** (blue line) and **MIP (C15-P)-peptide A** (red line) and **NIP-peptide A** (black line). **GFP-9**, **SAM** and **peptide A** were immobilized on the surface of QCM electrode. Frequency shifts were recorded upon injections of solutions of NPs into the sensor cells. (b) Competitive study of **MIP (C15-P)-GFP-9** interaction. **MIP(C15-P)** was preincubated with 0.1 mM **GFP-9** overnight. The mixture solution was injected into the sensor cells with **GFP-9** immobilized on the surface (black line). Binding was suppressed as compared to the **MIP (C15-P)** solution (pink line).

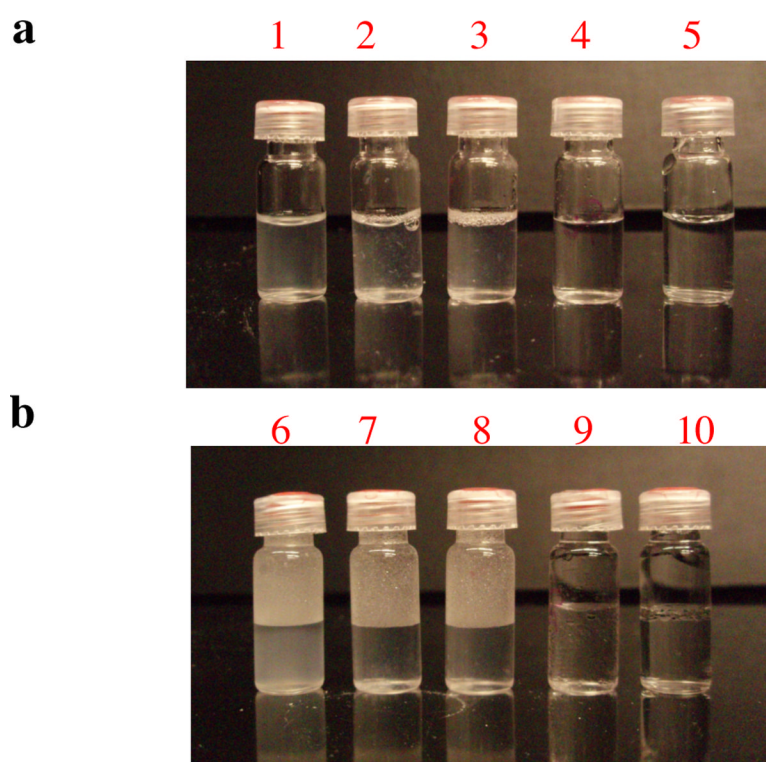


Figure 4. (a) 1 mL water with 1 mg Brij 30 (vial 1), 1mg **C15-P** (vial 2), 1mg **C13-P** (vial 3), 1mg **C5-P** (vial 4) and control (no peptide) (vial 5). (b) Mixed solvent (1mL water and 1mL hexane) with 1 mg Brij 30 (vial 6), 1mg **C15-P** (vial 7), 1mg **C13-P** (vial 8), 1mg **C5-P** (vial 9) and control (no peptide) (vial 10).